Segmentation of Enhanced Depth Imaging Optical Coherence Tomography Images Using Wavelet Based Graph Cut Algorithm

Abstract. Limited numbers of non-invasive imaging techniques are available for assessing the choroid, a structure that may be affected by a variety of retinal disorders or become primarily involved in conditions such as polypoidal choroidal vasculopathy and choroidal tumors. The introduction of enhanced depth imaging optical coherence tomography (EDI-OCT) has provided the advantage of in vivo cross-sectional imaging of the choroid, similar to the retina, with standard commercially available spectral domain OCT machines. A texture-based algorithm is introduced in this paper for fully automatic segmentation of choroidal images obtained from a 1060 nm optical coherence tomography (OCT) system. Dynamic programming is utilized to determine the location of the retinal pigment epithelium (RPE). The Bruch's membrane (BM) is the blood-retina barrier that separates the RPE cells of the retina from the choroid and can be segmented by searching for the pixels with the biggest gradient value below the RPE. A novel method is proposed to segment the choroid–sclera interface (CSI), which employs the wavelet based features to construct a Gaussian mixture model (GMM). The model is then used in a s-t cut graph for segmentation of the choroidal boundary. The proposed algorithm is compared with the manual segmentation and the results show an unsigned error of 1.71 ± 0.91 pixels for BM extraction and 7.65 ± 3.96 pixels for choroid detection.

Keywords— Enhanced Depth Imaging (EDI-OCT), Choroidal segmentation, Dynamic programming, Wavelet, Graph cut

978-1-4799-3163-7/13/$31.00 ©2013 IEEE

1. Introduction

Choroid is one of the eye structure layers located between the sclera and the retina. This pigmented layer contains many capillaries that supply feeding of the iris and retinal light receptor cells [1]. Many diseases such as polypoidal choroidal vasculopathy and choroidal tumors cause changes in the structure of this layer [2-4]; therefore segmentation of this layer has great importance. Optical Coherence Tomography (OCT) imaging of choroid layer is not possible due to signal transmission difficulty through retinal pigment epithelium (RPE) layer and increased depth of imaging [5]. Light source wavelength in OCT is 800 nanometers for retinal imaging, however for choroidal imaging a higher wavelength of approximately 1060 nanometer is required [6, 7]. By correction of standard technique in Spectral Domain (SD) OCT, choroid imaging is now possible with proper resolution using a new OCT imaging technique known as enhanced depth imaging (EDI) OCT [5]. Example of this imaging method is compared with conventional OCT in the Fig. 1.

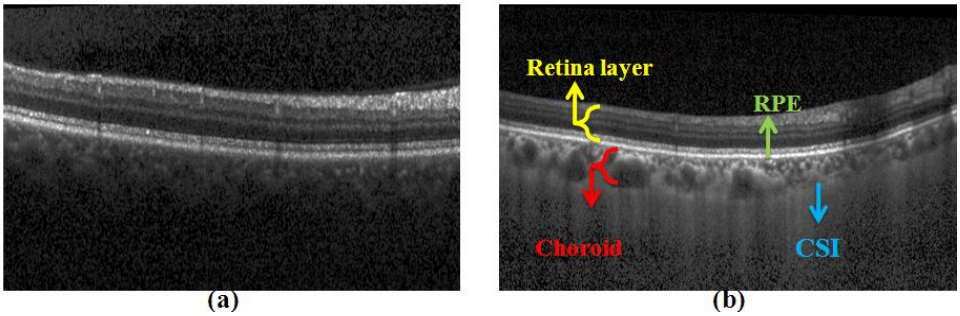

Fig. 1: An example of EDI OCT imagining (b), compared to conventional OCT (a)

In several studies, EDI OCT has been used to measure the thickness of the choroid, checking its relation with diseases, and monitoring the treatment process [8] In most of these studies, measurement of choroidal thickness is usually accomplished by manual labeling which is a time-consuming and tedious process. This problem is much more complicated especially when the number of studied population is numerous. Therefore in order to take advantage of EDI OCT, a segmentation algorithm should be developed. Only two studies have been conducted about automatic segmentation of these images, so far (Tian and Kajic [9, 10]). Many algorithms based on wavelet and graph-cut are already used in separation of retinal layers [11]. However due to heterogeneity in the choroid layers, such methods are not considered proper in choroid. Because of obvious difference between texture of choroid and other retinal layers, an algorithm based on texture classification can be effective. In this base we use a combination of graph-based methods and image features in wavelet-domain for choroidal segmentation.

2. Materials and methods

The proposed choroid segmentation method is tested on 50 two-dimensional EDI-OCT images obtained from Heidelberg 3D OCT-HRA2-KT device. Each dataset consisted of a SLO image and limited number of OCT scans with size of 496×768 (namely, for a data with 31 selected OCT slices, the whole data size would be 496×768×31). The OCT data is obtained from a 1060 OCT system by scanning over wide angle, which causes low signal strength on the image edges, especially towards the stack start and end, where the retina is narrow.

The proposed choroidal segmentation method in this paper consists of several steps. In first step, we apply boundary detection algorithm using dynamic programming to detect boundary of RPE layer which is the brightest part in retinal OCT images obtained from EDI OCT. Dynamic programming is a method based on optimality [12], which seeks best functions in which variables are not simultaneously in conjunction with one another. In simple problem of boundary tracking, the goal is to find the best path (least expensive) between one of possible starting points and one of possible ending points. In this step, upper bound of choroid which is the same as lower bound of RPE can be segmented. Fig. 2 shows the calculation stages of the cost function in this algorithm.

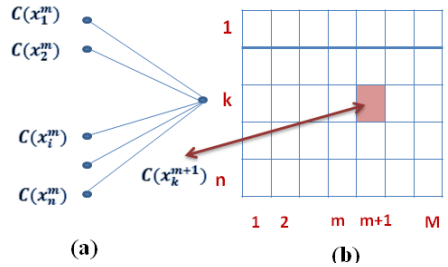

Fig. 2: Dynamic programming: (a) one step of cost calculation; (b) graph layers: marking nodes

In completion of optimization problem, following equation is considered.

$$\min(C(x^1, x^2, \dots, x^M)) = \min_{k=1,\dots,n}(C(x_k^M)) \quad (1)$$

where, x_k^M are ending point nodes, M is the number of graph layers between starting and ending points, $C(x^1, x^2, \dots, x^M)$ is the cost for the path between first and last point, and (M^{th}) represents graph layer. Last optimized path is obtained from the return path of the graph reviewed. Number of neighbors depends on the definition of adjacency and definition of the studied graph [13]. The Bruch's membrane (BM) can be located by searching for the pixels with the biggest gradient value below the RPE. Fig. 3 shows the result of BM segmentation for a sample EDI-OCT image.

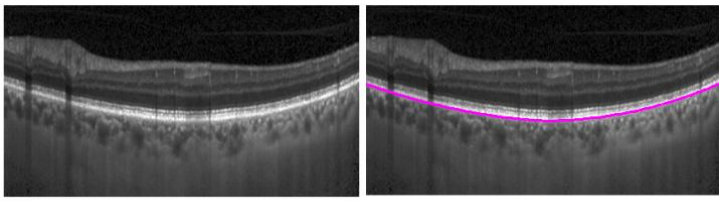

(a) (b)

Fig. 3 :(a) EDI-OCT image of the human eye.(b) The Bruch's Membrane

For discrimination of lower boundary of choroid (choroid–sclera interface (CSI)), a combination of algorithms is used. Texture descriptors can be used for segmentation of images consisting of several different textures [13]. Here we show how wavelet texture descriptors can be used for this purpose. Discrete wavelet transform - using filter bank and descriptors - is employed to extract image features. We use wavelet transform in order to calculate features for each pixel.
In other applications of wavelet transform for texture analysis, most prevalent features are wavelet energy signatures and their second-order statistics [14, 15]. In this case, Haar wavelet filters are used for the ease of use. Filter bank stages are repeated (multi-resolution approach), until no more extraction of new bands would be possible in the image. The energy of each high-pass filter at different stages of sub-bands and the energy of the last stage of the low-pass filter are extracted as image features.

Extracted features and a training image with a known segmentation are then used to construct a Gaussian Mixture Model (GMM) for the image.
GMM is a parametric pdf represented as a weighted sum of Gaussian component distributions. The idea for clustering with GMMs is the same as for k-means. We will make an initial guess for mean μ_k and covariance $\sum_k$, and then try to iteratively refine it. GMM parameters are estimated from training data using the iterative Expectation-Maximization (EM) algorithm which is a well established algorithm for fitting a mixture model to a set of training data. Each of extracted descriptors is assumed to have normal distribution and its parameters including mean and covariance are calculated using GMM. Gaussian pdfs of each image labels are used in graph creation and final segmentation.
The algorithm should take an unknown image and segment it using the learned model. Graph cut segmentation is constructed based on the learned model to obtain spatially coherent segmentation.
Direct use of mixed optimization algorithms of minimum-cut/maximum flow was first introduced by Greig [16] in image processing of binary images. Using graph optimization algorithms, a powerful method of optimal bordering and region classification in N-dimensional image data was proposed [17]. This method starts by one or more object indicator points and one or more field indicator points, using interactive or automatic identification. These points are called seeds, and are classified as hard constraint.

Moreover soft constraints reflect boundaries or regional data (Fig. 4). The overall shape of cost function C is represented as follows [18].

$$C(f) = c_{data}(f) + c_{smoot\,h}(f) \quad (2)$$

Minimum s-t cut problem, could be solved through finding a maximum flow from source (s) to sink (t). In maximum flow algorithm, maximum amount of water to sink is delivered using directed arc graphs and the amount of water flow through each separate arc is determined using arc capacity or cost. The greatest amount of maximum flow from s to t, saturates a set of graph arcs. These saturated arcs, divide nodes into two separate sections of S and T, related to minimum cuts [13, 19].
In extraction of choroid area, $c_{data}(f)$ is the distance between each image pixel to initial sample class made by GMM. $c_{smoot\,h}(f)$ is a matrix of costs which is related to adjacent pixel values. In this work, we assigned a fixed valued matrix with zeros on diagonal as $c_{smoot\,h}(f)$. The increase in fixed term would enhance adjacency constraint constant and therefore would result in a finer separation.

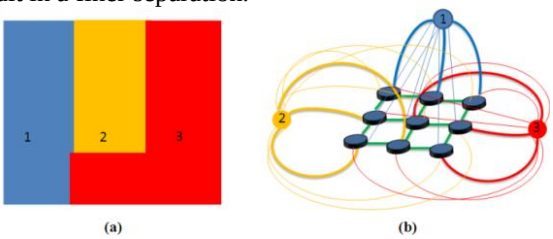

Fig. 4: Graph Cut Classification - example of simple Classification. (a) Image with 3 classes. (b) Related graph and s-t nodes.

3. Results

The proposed method is tested on 50 EDI-OCT images obtained from Heidelberg 3D OCT-HRA2-KT device. For evaluation of the proposed method, manual segmentation of two observers were used as the gold standard and an unsigned error (mean± std) of 1.71±0.91 pixels and 7.65±3.96 pixels were obtained in detection of RPE and CSI, respectively. Fig. 5 demonstrates two samples showing performance of the proposed method.

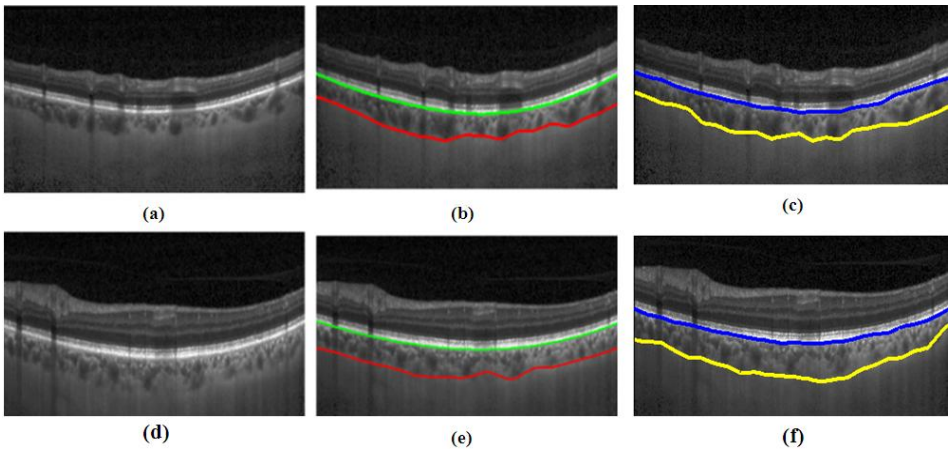

Fig. 5: :(a),(d) EDI-OCT image,(b),(e) our algorithm, (c), (f) manual segmentation

For validation purpose, the mean signed and unsigned border positioning errors for each border were compared manual segmentation and are presented in Tables I and II for each boundary.

According to Tables I and II, the border positioning errors between the proposed algorithm and the reference standard were similar to those computed between the observers. For example, the algorithm's overall unsigned error were 1.71±0.91 pixels and 7.65±3.96 pixels for BM and CSI, respectively; while the overall observer error were 1.91±0.93 pixels and 8.95±4.53 pixels for BM and CSI, respectively. The border positioning errors of the proposed method show significant improvement.

TABLE I
SUMMARY OF MEAN SIGNED BORDER POSITIONING ERRORS (MEAN ± SD)

	Avg. Obs. Vs. Our Alg.	**Obs. 1 Vs. Obs. 2**
RPE	0.86-±0.52	1.41±0.81
Choroid	4.11±2.41	7.35±5.08

TABLE II
SUMMARY OF MEAN UNSIGNED BORDER POSITIONING ERRORS (MEAN ± SD)

Border	**Avg. Obs. vs. Our Alg.**	**Obs. 1 vs. Obs. 2**
RPE	1.71±0.91	1.91±0.93
choroid	7.65±3.96	8.95±4.53

4. Conclusion

In this paper a novel method is proposed for choridal segmentation in EDI-OCT images employing wavelet based features to construct a Gaussian mixture model. The model is then used in a s-t cut graph for segmentation of the choroidal boundary. The algorithm is robust even in presence of speckle noise, low signal (thin choroid), shadowing and other artifacts. In conclusion, the new method seems to have important advantage over older methods which makes the accuracy of the method higher than other choroid segmentation approaches. The performance of the method is fast and the implementation is relatively simple in comparison to more complicated algorithms.
The proposed algorithm in this paper is applied on 2D EDI-OCT images. We are working to extend this algorithm for whole 3D EDI-OCT images which could be led to preparation of more useful information for ophthalmologists like a thickness map for choroidal area.

References

[1] G. A. Cioffi, E. Granstam, and A. Alm, "" Ocular Circulation" in Adler's Physiology of the Eye," 2003.

[2] G. Barteselli, J. Chhablani, S. El-Emam, H. Wang, J. Chuang, I. Kozak, *et al.*, "Choroidal Volume Variations with Age, Axial Length, and Sex in Healthy Subjects: A Three-Dimensional Analysis," *Ophthalmology,* vol. 119, pp. 2572-2578, 12// 2012.

[3] S. E. Chung, S. W. Kang, J. H. Lee, and Y. T. Kim, "Choroidal thickness in polypoidal choroidal vasculopathy and exudative age-related macular degeneration," *Ophthalmology,* vol. 118, pp. 840-845, 2011.

[4] J. Yeoh, W. Rahman, F. Chen, C. Hooper, P. Patel, A. Tufail, *et al.*, "Choroidal imaging in inherited retinal disease using the technique of enhanced depth imaging optical coherence tomography," *Graefe's Archive for Clinical and Experimental Ophthalmology,* vol. 248, pp. 1719-1728, 2010.

[5] R. F. Spaide, H. Koizumi, and M. C. Pozonni, "Enhanced depth imaging spectral-domain optical coherence tomography," *American journal of ophthalmology,* vol. 146, pp. 496-500, 2008.

[6] R. F. Spaide, "Enhanced depth imaging optical coherence tomography of retinal pigment epithelial detachment in age-related macular degeneration," *American journal of ophthalmology,* vol. 147, pp. 644-652, 2009.

[7] B. Považay, B. Hermann, A. Unterhuber, B. Hofer, H. Sattmann, F. Zeiler, *et al.*, "Three-dimensional optical coherence tomography at 1050nm versus 800nm in retinal pathologies: enhanced performance and choroidal penetration in cataract patients," *Journal of biomedical optics,* vol. 12, pp. 041211-041211-7, 2007.

[8] T. Fujiwara, Y. Imamura, R. Margolis, J. S. Slakter, and R. F. Spaide, "Enhanced depth imaging optical coherence tomography of the choroid in highly myopic eyes," *American journal of ophthalmology*, vol. 148, pp. 445-450, 2009.

[9] J. Tian, P. Marziliano, M. Baskaran, T. A. Tun, and T. Aung, "Automatic measurements of choroidal thickness in EDI-OCT images," in *Engineering in Medicine and Biology Society (EMBC), 2012 Annual International Conference of the IEEE*, 2012, pp. 5360-5363.

[10] V. Kajić, M. Esmaeelpour, B. Považay, D. Marshall, P. L. Rosin, and W. Drexler, "Automated choroidal segmentation of 1060 nm OCT in healthy and pathologic eyes using a statistical model," *Biomedical Optics Express*, vol. 3, pp. 86-103, 2012.

[11] M. K. Garvin, M. D. Abràmoff, R. Kardon, S. R. Russell, X. Wu, and M. Sonka, "Intraretinal layer segmentation of macular optical coherence tomography images using optimal 3-D graph search," *Medical Imaging, IEEE Transactions on*, vol. 27, pp. 1495-1505, 2008.

[12] R. E. Bellman and S. E. Dreyfus, "Applied dynamic programming," 1962.

[13] M. Sonka, V. Hlavac, and R. Boyle, "Image processing, analysis, and machine vision," 1999.

[14] S. Arivazhagan and L. Ganesan, "Texture classification using wavelet transform," *Pattern Recognition Letters*, vol. 24, pp. 1513-1521, 2003.

[15] G. Van de Wouwer, P. Scheunders, and D. Van Dyck, "Statistical texture characterization from wavelet representations," *IEEE Trans. Image Process. v8*, pp. 592-598.

[16] D. Greig, B. Porteous, and A. H. Seheult, "Exact maximum a posteriori estimation for binary images," *Journal of the Royal Statistical Society. Series B (Methodological)*, pp. 271-279, 1989.

[17] Y. Boykov and G. Funka-Lea, "Graph cuts and efficient ND image segmentation," *International Journal of Computer Vision*, vol. 70, pp. 109-131, 2006.

[18] S. Geman and D. Geman, "Stochastic relaxation, Gibbs distributions, and the Bayesian restoration of images," *Pattern Analysis and Machine Intelligence, IEEE Transactions on*, pp. 721-741, 1984.

[19] A. V. Goldberg and R. E. Tarjan, "A new approach to the maximum-flow problem," *Journal of the ACM (JACM)*, vol. 35, pp. 921-940, 1988.